PERGAMON

International Journal of Solids and Structures 39 (2002) 1131–1144

INTERNATIONAL JOURNAL OF SOLIDS and STRUCTURES

www.elsevier.com/locate/ijsolstr

Wave propagation in piezoelectric coupled plates by use of interdigital transducer. Part 2: Wave excitation by interdigital transducer

Q. Wang [a,*], V.K. Varadan [b]

[a] *Department of Civil Engineering, National University of Singapore, Block E1A, #07-03, 1 Engineering Drive 2, Singapore 119260, Singapore*

[b] *Department of Engineering Science and Mechanics, The Pennsylvania State University, University Park, PA 16802, USA*

Received 24 May 2001

Abstract

In the second part of the research on wave propagation in the piezoelectric coupled plate by interdigital transducer (IDT), the analytical model of the wave excitation by IDT with both infinite and finite length is derived the first time. This work is an extension of the research on the application of IDT in the piezoelectric media, which is mainly used in time delay device. The extension of the research can provide an analytical solution for the wave excitation by IDT in a metal substrate surface bonded by a piezoelectric layer. Such solution may have practical values in many fields, i.e. the health monitoring of structures. In addition, such an extension enables the piezoelectric coupling effects fully modelled in the mathematical model. The analysis is based on the type of surface wave solution discussed in Part 1 of the research paper. The derivation of the solution for the case of infinitely long IDT is under a hypothesis of certain configuration of the IDT wavelength. The validity of the hypothesis is verified for most of IDT wavelength designs. The analysis of the wave propagation by use of a finitely long IDT is further obtained by Fourier transform. The mathematical analysis shows that the wave propagation excited by the IDT is exactly the surface wave which was studied in Part 1 [Int. J. Solids Struct., 39, 1119–1130] of the research. Hence, the analytical solution of the wave propagation in the piezoelectric coupled plate is derived, which reveals the surface wave propagating in the structure. This theoretical research is useful for the application of health monitoring of structures by IDT, and may be used as the framework for the design of IDT in wave excitation of smart structures.

Keywords: Piezoelectric coupled plate; Interdigital transducer; Dispersion characteristics; Wave phase velocity; Health monitoring of structures

1. Introduction

A practical interdigital transducer (IDT) with finite length bonded by a metal plate is shown in Fig. 1. IDT is a thin piezoelectric film surface bonded on either piezoelectric or unpiezoelectric substrate for the

* Corresponding author. Tel.: +65-874-4683; fax: +65-779-1635.
E-mail address: cvewangq@nus.edu.sg (Q. Wang).

0020-7683/02/$ - see front matter
PII: S0020-7683(01)00244-X

use of wave excitation or reception of structures. On the surface of the wafer, a pattern of electrodes is designed, which comprises two alternating sets of fingers which are connected to external electric power sources for the energy supply. As introduced in Part 1 of the paper, IDT was first used to excite the surface wave (SAW) devices in radar communication equipment as filters and delay lines, and some consumer areas such as pagers, mobile phones and sensors (Morgan, 1998; Campbell, 1998; White, 1998). It also has large potential in separating, amplifying and storing signals and in other signal processing applications in acoustoelectronics (Auld, 1973a,b; Parton and Kudryavtser, 1988). This device is recently found to have large potential to be used as attractive sensors for various physical variables, such as force, electric fields, magnetic fields, temperature, pressure, etc. (Varadan and Varadan, 2000).

Although there are considerable researches on the subject of analysis of IDT, the analytical solution for the wave excitation by IDT is still unsolved completely. Most of the previous work attempted at this issue by combining analytical and numerical methods as clearly stated by Milsom et al. (1977). The difficulties of the analyses lie in the full electromechanical coupling in the structure. Tseng (1968), Coquin and Tierstan (1967) and Joshin and White (1969) analysed this problem by solving an electrostatic problem, and substituted the distribution of the electric fields into the electromechanical coupled equation and hence obtained the secondary electric fields and the distribution of displacement fields. In the monograph of Parton and Kudryavtser (1988), the analytical solutions for an IDT which generates Rayleigh surface waves in a hexagonal 6 mm piezoelectric medium was presented based on the same procedure. However, they could not fully model the piezoelectric effects in their models. Another popular analysis proposed by Balakrirev and Gilinskii (1982) is to use Green matrix method to solve a two-dimensional (2D) problem for a half unbounded crystal. This method provided a situation where there is only a unit linear charge on the

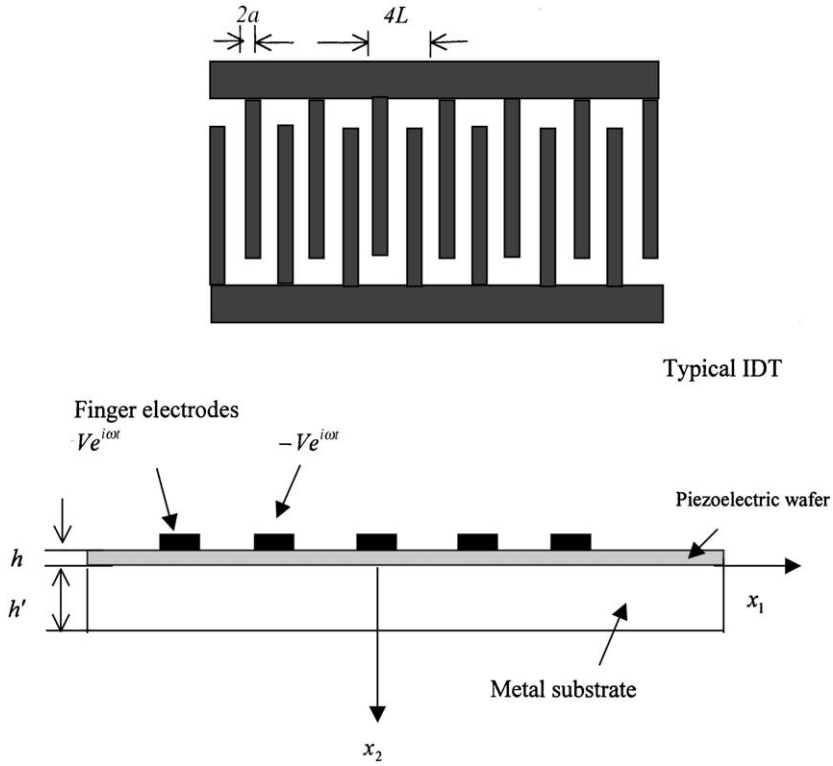

Fig. 1. Piezoelectric coupled plate surface bonded by IDT.

boundary. However, in practice, the method is hardly feasible for an arbitrary crystal due to the difficulties in constructing the Green matrix. Some recent progresses are contributed by the finite element method (Hasegawa and Koshiba, 1990; Yong et al., 1998; Xu, 2000), the boundary element method (Hashimoto and Yamaguchi, 1991), and 2D's Green function (Huang and Paige, 1998). However, the behaviour of SAW by IDT still cannot be predicted accurately and modelled analytically. Ogilvy (1996) presented an approximate analysis for predicting the generation of elastic waves by IDT in multi-layered piezoelectric materials. However, neither the width of the IDT fingers nor the dimensions of the IDT are explicitly taken into account. All the solutions for the above mentioned applications of IDT are focused on the wave propagation in a piezoelectric medium surface bonded by a metal layer (Zhang et al., 1993; Ventura et al., 1995; Morgan, 1985).

As mentioned in the first part of the paper, the applications by IDT in the health monitoring of structures have been attempted (Badcock and Birt, 2000; Monkhouse et al., 2000). In this new application of IDT, the structure to be studied mainly consists of the metal substrate surface bonded by a piezoelectric layer used to excite wave propagation in this piezoelectric coupled structure. Such new potential of IDT provides a challenge for the research on the wave excitation by IDT in the piezoelectric coupled structure mentioned in the previous paragraph. An extension for the research on the wave propagation by IDT in piezoelectric structures is expected to provide an accurate mathematical model to couple the piezoelectric coupling effects fully.

The purpose of this paper is to derive an analytical solution for SH wave propagation excited by IDT in a piezoelectric coupled plate. The dispersion characteristics of the wave propagation have already been discussed in Part 1 of the paper based on the type of surface wave solution. The mathematical governing equation and corresponding boundary conditions for the analytical solution for the wave excitation are provided with infinitely long IDT modelled first. A hypothesis on the wavelength of IDT is discussed for the deduction of the analytical solution and verified. The analytical analysis of the wave propagation with a finitely long IDT is further obtained by Fourier transform. The derivation of the analytical solution for the wave propagation in the piezoelectric coupled structure by IDT is important in the design of IDT in the health monitoring of structures and other engineering applications.

2. Mechanics model of wave propagation by use of IDT

An IDT was deposited on the piezoelectric coupled plate shown in Fig. 1. An electric voltage is hence provided across the electrodes producing an alternative electric field in the materials and causing wave propagation of the same frequency in the piezoelectric coupled plate.

The dispersion characteristics of the SH wave propagation in this structure has been studied in the first part of the paper, and the type of SAW solution has been presented. In this part, the wave excitation by use of IDT will be studied hereafter.

As the solutions for the deflection and shear stress of the metal core, the deflection, the electric potential and the shear stress of the piezoelectric layer have already been obtained in Eqs. (13), (17)–(23) in the first part of the research, the following deductions will be shown without repeating the same procedures in the first part of the research paper.

According to the coordinate system in Fig. 1, since the IDT is infinite length and the period of electric field in x_1 is $4L$ due to the wavelength of IDT, the above displacement solution for metal part can be expressed in form of series as,

$$u_3' = \sum_{i=i_1}^{\infty} \left(C_{1i} e^{-\chi_i' x_2} + C_{2i} e^{\chi_i' x_2} \right) e^{i(\omega t - k_i x_1)} \tag{1}$$

where

$$k_i = \frac{\pi}{L}\left(i+\frac{1}{2}\right), \quad \gamma_i' = k_i\sqrt{1-\left(\frac{\omega}{k_i v'}\right)^2}, \quad i_1 = \left[\frac{\omega}{v'}\frac{L}{\pi}-\frac{1}{2}\right]$$

The symbol $[\cdot]$ means the integer part of a number. From the expression of i_1, it can be seen the condition of $\omega/k_i < v'$ is satisfied, which means the surface wave solution is employed in the discussion as stated in Part 1 of the research.

Similarly, the deflection of the piezoelectric layer can be expressed as follows based on the solutions in Part 1,

$$u_3 = \sum_{i=I}^{\infty}(A_{1i}e^{-\gamma_i x_2} + A_{2i}e^{\gamma_i x_2})\exp\left(i\omega\left(t-\frac{k_i x_1}{\omega}\right)\right) \quad \text{when } \frac{\omega}{k_i} < v, v' \tag{2}$$

$$u_3 = \sum_{i=i_1}^{i_2}(A_{1i}\cos\gamma_i x_2 + A_{2i}\sin\gamma_i x_2)\exp\left(i\omega\left(t-\frac{k_i x_1}{\omega}\right)\right) \quad \text{when } v' > \frac{\omega}{k_i} > v \tag{3}$$

where

$$\gamma_i = k_i\sqrt{\left|1-\left(\frac{\omega}{k_i v}\right)^2\right|}, \quad v^2 = \frac{\bar{c}_{44}}{\rho}, \quad i_2 = \left[\frac{\omega}{v}\frac{L}{\pi}-\frac{1}{2}\right], \quad I = \max(i_1, i_2)$$

According to Eqs. (19) and (20) in Part 1, the electric potential is obtained,

$$\phi = \sum_{i=I}^{\infty}\left[\left(B_{1i}e^{-k_i x_2} + B_{2i}e^{k_i x_2}\right) + \frac{e_{15}}{\Xi_{11}}(A_{1i}e^{-\gamma_i x_2} + A_{2i}e^{\gamma_i x_2})\right]\exp\left(i\omega\left(t-\frac{k_i x_1}{\omega}\right)\right) \quad \text{if } \frac{\omega}{k_i} < v, v' \tag{4}$$

$$\phi = \sum_{i=i_1}^{i_2}\left[\left(B_{1i}e^{-k_i x_2} + B_{2i}e^{k_i x_2}\right) + \frac{e_{15}}{\Xi_{11}}(A_{1i}\cos\gamma_i x_2 + A_{2i}\sin\gamma_i x_2)\right]\exp\left(i\omega\left(t-\frac{k_i x_1}{\omega}\right)\right) \quad \text{if } v' > c > v \tag{5}$$

The electric displacement is thus obtained by

$$D_2 = e_{15}\frac{\partial u_3}{\partial x_2} - \Xi_{33}\frac{\partial\phi}{\partial x_2} = \sum_{i=I}^{\infty} -\Xi_{11}k_i(-B_{1i}e^{-k_i x_2} + B_{2i}e^{k_i x_2})\exp\left(i\omega\left(t-\frac{k_i x_1}{\omega}\right)\right) \quad \text{if } \frac{\omega}{k_i} < v, v' \tag{6}$$

$$D_2 = \sum_{i=i_1}^{i_2} -\Xi_{11}k_i(-B_{1i}e^{-k_i x_2} + B_{2i}e^{k_i x_2})\exp\left(i\omega\left(t-\frac{k_i x_1}{\omega}\right)\right) \quad \text{if } v' > c > v \tag{7}$$

The shear stress in the metal core is expressed as follows from Eq. (21) in Part 1,

$$\sigma_{23}' = \sum_{i=I}^{\infty} c_{44}'\left[(-\gamma_i')C_{1i}e^{-\gamma_i' x_2} + \gamma_i' C_{2i}e^{\gamma_i' x_2}\right]\exp\left(i\omega\left(t-\frac{k_i x_1}{\omega}\right)\right) \tag{8}$$

The shear stress in the piezoelectric layer is shown from Eqs. (22) and (23) from Part 1,

$$\sigma_{23} = \sum_{i=I}^{\infty}\left[(-\gamma_i)\bar{c}_{44}(A_{1i}e^{-\gamma_i x_2} - A_{2i}e^{\gamma_i x_2}) + (-k_i)e_{15}\left(B_{1i}e^{-k_i x_2} - B_{2i}e^{k_i x_2}\right)\right]\exp\left(i\omega\left(t-\frac{k_i x_1}{\omega}\right)\right) \quad \text{if } \frac{\omega}{k_i} < v, v' \tag{9}$$

and

$$\sigma_{23} = \sum_{i=i_1}^{i_2} \left[(-\chi_i)\bar{c}_{44}(A_{1i}\sin\chi_i x_2 - A_{2i}\cos\chi_i x_2) + (-k_i)e_{15}\left(B_{1i}e^{-k_i x_2} - B_{2i}e^{k_i x_2}\right)\right] \exp\left(i\omega\left(t - \frac{k_i x_1}{\omega}\right)\right)$$
$$\text{if } v' > c > v \tag{10}$$

The potential ϕ' in the vacuum can be derived by solving the electronic Maxwell equation,

$$\nabla^2\phi' = 0 \tag{11}$$

Such solution for ϕ' and D' can be obtained as follows when seeking the solution which remains finite as $x_2 \to -\infty$:

$$\phi' = \sum_{i=0}^{\infty} F_i e^{k_i x_2} \exp\left(i\omega\left(t - \frac{k_i x_1}{\omega}\right)\right) \tag{12}$$

$$D' = \sum_{i=0}^{\infty} -\Xi_0 k_i F_i e^{k_i x_2} \exp\left(i\omega\left(t - \frac{k_i x_1}{\omega}\right)\right) \tag{13}$$

The above mathematical model can be solved analytically together with the following boundary conditions, at $x_2 = 0$:

$$u_3 = u_3' \tag{14}$$

$$\sigma_{23} = \sigma_{23}' \tag{15}$$

$$\phi = 0 \tag{16}$$

at $x_2 = -h$:

$$\sigma_{23} = 0 \tag{17}$$

$$\phi = \phi' \tag{18}$$

$$D_2 = D' \text{ (outside electrodes)} \tag{19}$$

$$\phi = \phi' = V \text{ (inside electrodes)} \tag{20}$$

at $x_2 = h'$:

$$\sigma_{23}' = 0 \tag{21}$$

The analytical solution for the wave propagation in the piezoelectric coupled plate with infinitely long IDT and finitely long IDT will be given in the following sections separately.

3. Analytical solutions for wave propagation with infinitely long IDT

The deflection, electric potential and stress in the piezoelectric layer are expressed by Eqs. (2), (4) and (9) irrelevant of the comparison of the bulk shear wave velocities of the metal substrate and the piezoelectric layer. Nevertheless, Eqs. (3), (5) and (10) are only valid for the case that the bulk shear wave velocity of the host metal plate is larger than that of the piezoelectric layer. In order to obtain the analytical solution for the above mathematical model given in the previous section, a hypothesis on IDT wavelength is provided, i.e. $I = \max(i_1, i_2) = 0$. This hypothesis reveals the fact that the all the solutions of the physical variables in the piezoelectric layer will follow Eqs. (2), (4) and (9) by proper design of the basic wave number $k_0 = \pi/2L$,

i.e. the design of wavelength of IDT. Taking steel-PZT 4 piezoelectric coupled plate as an example, the bulk shear wave velocity of steel and PZT 4 are about $v|_{\text{steel}} = 3281$ m/s, $v|_{\text{PZT 4}} = 2351$ m/s. If the frequency of the excitation voltage is used as 1.4 MHz applied to the IDT. The hypothesis of $I = 0$ requires $L < 5.5$ mm, which means the wavelength of IDT is 2.2 cm. Such requirement is satisfied by most of the designs of IDT wavelength. When gold-PZT 4 is employed in the estimations, it shows that the wavelength of the standard electrode pattern is around 1.1 cm which can also be satisfied in most of the designs of the IDT. Upon the above observations, the hypothesis of using Eqs. (2), (4) and (9) for the solutions of wave propagation in the piezoelectric layer is thus reasonable and valid for most of the IDT designs, and will be used in the following analysis. It is noted that all the above analyses are based on the surface wave solution assumed in the piezoelectric layer. The wave excitation of other types of the wave solutions by IDT is beyond the scope of this paper.

Boundary conditions expressed in Eqs. (14)–(21) are rewritten as follows when the solutions in the metal substrate, the piezoelectric layer, and the vacuum are taken from the preceding analyses:

$$\sum_{i=0}^{\infty}(C_{1i}+C_{2i})\mathrm{e}^{\mathrm{i}k_i x} = \sum_{i=0}^{\infty}(A_{1i}+A_{2i})\mathrm{e}^{\mathrm{i}k_i x_1} \tag{22}$$

$$\sum_{i=0}^{\infty}(-\chi_i)\bar{c}_{44}(A_{1i}-A_{2i}) + (-k_i)\mathrm{e}_{15}(B_{1i}-B_{2i})\mathrm{e}^{\mathrm{i}k_i x_1} = \sum_{i=0}^{\infty}(-\chi_i')c_{44}'(C_{1i}-C_{2i})\mathrm{e}^{\mathrm{i}k_i x_1} \tag{23}$$

$$\sum_{i=0}^{\infty}\left(B_{1i}+B_{2i}+\frac{\mathrm{e}_{15}}{\Xi_{11}}(A_{1i}+A_{2i})\right)\mathrm{e}^{\mathrm{i}k_i x_1} = 0 \tag{24}$$

$$\sum_{i=0}^{\infty}((-\chi_i)\bar{c}_{44}(A_{1i}\mathrm{e}^{\chi_2 h}-A_{2i}\mathrm{e}^{-\chi_2 h}) + (-k_i)\mathrm{e}_{15}(B_{1i}\mathrm{e}^{\chi_1 h}-B_{2i}\mathrm{e}^{-\chi_1 h}))\mathrm{e}^{\mathrm{i}k_i x_1} = 0 \tag{25}$$

$$\sum_{i=0}^{\infty}\left(\left(B_{i1}\mathrm{e}^{\chi_1 h}+B_{2i}\mathrm{e}^{-\chi_1 h}\right)+\frac{\mathrm{e}_{15}}{\Xi_{11}}\left(A_{1i}\mathrm{e}^{\chi_2 h}+A_{2i}\mathrm{e}^{-\chi_2 h}\right)\right)\mathrm{e}^{\mathrm{i}k_i x_1} = \sum_{i=0}^{\infty}F_i\mathrm{e}^{-k_i h}\mathrm{e}^{\mathrm{i}k_i x_1} \tag{26}$$

$$\sum_{i=0}^{\infty}(-\Xi_{11}(-k_i B_{1i}\mathrm{e}^{k_i h}+k_i B_{2i}\mathrm{e}^{-k_i h})+\Xi_0 k_i F_i\mathrm{e}^{-k_i h})\mathrm{e}^{\mathrm{i}k_i x_1} = 0 \quad a < x_1 < L \tag{27}$$

$$\sum_{i=0}^{\infty}F_i\mathrm{e}^{-k_i h}\mathrm{e}^{\mathrm{i}k_i x_1} = 0 \quad 0 < x_1 < a \tag{28}$$

$$\sum_{i=0}^{\infty}\left(C_{1i}\mathrm{e}^{-\chi' h'}-C_{2i}\mathrm{e}^{\chi' h'}\right) = 0 \tag{29}$$

The mathematics solution for all the seven non-zero coefficients C_{1i}, C_{2i}, A_{1i}, A_{2i}, B_{1i}, B_{2i}, F_i $(i = 1, 2, \ldots, \infty)$ will be obtained from Eqs. (22)–(29).

From Eq. (29), we have

$$C_{1i} = C_{2i}\mathrm{e}^{2\chi' h'} \tag{30}$$

Substituting the above expressions in Eqs. (22)–(24) yield the following relations,

$$A_{1i}+A_{2i} = -\frac{\Xi_{11}}{\mathrm{e}_{15}}(B_{1i}+B_{2i}) \tag{31}$$

$$A_{1i} - A_{2i} = G_{1i}B_{1i} + G_{2i}B_{2i} \tag{32}$$

where

$$G_{1i} = -\frac{k_i e_{15}}{\chi_i \bar{c}_{44}} - \frac{\chi_i' c_{44}'}{\chi_i \bar{c}_{44}} \frac{\Xi_{11}}{e_{15}} \frac{e^{2\chi' h'} - 1}{e^{2\chi' h'} + 1}, \qquad G_{2i} = \frac{k_i e_{15}}{\chi_i \bar{c}_{44}} - \frac{\chi_i' c_{44}'}{\chi_i \bar{c}_{44}} \frac{\Xi_{11}}{e_{15}} \frac{e^{2\chi' h'} - 1}{e^{2\chi' h'} + 1}$$

Thus A_{1i} and A_{2i} are obtained from the above equations as,

$$A_{1i} = H_{1i}B_{1i} + H_{2i}B_{2i} \tag{33}$$

$$A_{2i} = H_{3i}B_{1i} + H_{4i}B_{2i} \tag{34}$$

where

$$H_{1i} = \frac{1}{2}\left(G_{1i} - \frac{\Xi_{11}}{e_{15}}\right), \quad H_{2i} = \frac{1}{2}\left(G_{2i} - \frac{\Xi_{11}}{e_{15}}\right), \quad H_{3i} = -\frac{1}{2}\left(G_{1i} + \frac{\Xi_{11}}{e_{15}}\right), \quad H_{4i} = -\frac{1}{2}\left(G_{2i} + \frac{\Xi_{11}}{e_{15}}\right)$$

Substituting Eqs. (33) and (34) into Eqs. (25) and (26) yields,

$$\left(H_{1i}e^{\chi_i h} - H_{3i}e^{-\chi_i h} + \frac{k_i e_{15}}{\chi_i \bar{c}_{44}} e^{k_i h}\right)B_{1i} + \left(H_{2i}e^{\chi_i h} - H_{4i}e^{-\chi_i h} - \frac{k_i e_{15}}{\chi_i \bar{c}_{44}} e^{k_i h}\right)B_{2i} = 0 \tag{35}$$

i.e.

$$J_{1i}B_{1i} + J_{2i}B_{2i} = 0 \tag{36}$$

$$\left(e^{k_i h} + \frac{e_{15}}{\Xi_{11}}H_{1i}e^{\chi_i h} + \frac{e_{15}}{\Xi_{11}}H_{3i}e^{-\chi_i h}\right)B_{1i} + \left(e^{-k_i h} + \frac{e_{15}}{\Xi_{11}}H_{2i}e^{\chi_i h} + \frac{e_{15}}{\Xi_{11}}H_{4i}e^{-\chi_i h}\right)B_{2i} = F_i e^{-k_i h} \tag{37}$$

i.e.

$$J_{3i}B_{1i} + J_{4i}B_{2i} = F_i e^{-k_i h} \tag{38}$$

The coefficients B_{1i} and B_{2i} can thus be expressed in terms of F_i as follows:

$$B_{1i} = \frac{F_i e^{-k_i h}}{J_{3i} - \frac{J_{1i}}{J_{2i}}J_{4i}} \tag{39}$$

$$B_{2i} = \frac{F_i e^{-k_i h}}{J_{4i} - \frac{J_{2i}}{J_{1i}}J_{3i}} \tag{40}$$

Substituting the above two expressions into Eq. (27) gives,

$$\sum_{i=0}^{\infty} k_i F_i e^{-k_i h}\left(\Xi_0 + \frac{\Xi_{11}e^{k_i h}}{J_{3i} - \frac{J_{1i}}{J_{2i}}J_{4i}} - \frac{\Xi_{11}e^{-k_i h}}{J_{4i} - \frac{J_{2i}}{J_{1i}}J_{3i}}\right)e^{ik_i x_1} = 0 \quad a < x_1 < L \tag{41}$$

By defining

$$\overline{F}_i = F_i e^{-k_i h}\left(\Xi_0 + \frac{\Xi_{11}e^{k_i h}}{J_{3i} - \frac{J_{1i}}{J_{2i}}J_{4i}} - \frac{\Xi_{11}e^{-k_i h}}{J_{4i} - \frac{J_{2i}}{J_{1i}}J_{3i}}\right) \tag{42}$$

Eqs. (28) and (41) may be rearranged as

$$\sum_{i=0}^{\infty} \overline{F}_i e^{ik_i x_1} = 0 \quad 0 < x_1 < a \tag{43}$$

$$\sum_{i=0}^{\infty} k_i \overline{F}_i (1 + L_i) e^{ik_i x_1} = V \quad a < x_1 < L \tag{44}$$

where

$$L_i = \left(\Xi_K + \frac{\Xi_{11} e^{k_i h}}{R_{1i} - \frac{Q_{1i}}{Q_{2i}} R_{2i}} - \frac{\Xi_{11} e^{-k_i h}}{R_{2i} - \frac{Q_{2i}}{Q_{1i}} R_{1i}} \right)^{-1} - 1$$

Rewriting Eqs. (43) and (44) in their real function forms gives,

$$\sum_{i=0}^{\infty} \overline{F}_i \cos\left(i + \frac{1}{2}\right)\bar{x} = 0 \quad \bar{a} < \bar{x} < \pi \tag{45}$$

$$\sum_{i=0}^{\infty} \left(i + \frac{1}{2}\right) \overline{F}_i (1 + L_i) \cos\left(i + \frac{1}{2}\right)\bar{x} = V \quad 0 < \bar{x} < \bar{a} \tag{46}$$

where $\bar{x} = \pi x_1 / L$, $\bar{a} = \pi a / L$.

The solutions for Eqs. (45) and (46) can be obtained from an infinite system of linear algebraic equations (Bateman and Erdelyi, 1955; Parton and Kudryavtser, 1988).

The set of equations are given as,

$$\overline{F}_i = \frac{V P_i(\cos \bar{a})}{\left(i + \frac{1}{2}\right) K\left(\cos \frac{\bar{a}}{2}\right)} - \sum_{n=0}^{\infty} \overline{F}_n L_n \beta_{ni} \quad (i = 1, 2, \ldots, \infty) \tag{47}$$

where

$$\beta_{ni} = \left(i + \frac{1}{2}\right) \int_0^{\pi} P_n(\cos \xi) P_i(\cos \xi) \sin \xi \, d\xi \tag{48}$$

$$P_i(\cos \xi) = \frac{\sqrt{2}}{\pi} \int_0^{\xi} \frac{\cos\left(i + \frac{1}{2}\right)x \, dx}{\sqrt{\cos x - \cos \xi}} \tag{49}$$

$$K\left(\cos \frac{\xi}{2}\right) = \sum_{i=0}^{\infty} \frac{P_i(\cos \xi)}{\left(i + \frac{1}{2}\right)} \tag{50}$$

$P_i(\cos \xi)$ in the above equation is the standard integral representation for Legendre polynomial and $K(\cos \xi/2)$ is the full elliptic integral of the first kind (Bateman and Erdelyi, 1955).

If the finite N terms are used in Eq. (47) on the condition that the convergence of the solution is ensured by the Legendre polynomial theory, the result of the coefficients $\overline{F}_i$ $(i = 1, 2, \ldots, N)$ can thus be obtained from the following equation:

$$[L]\{\overline{F}\} = \frac{V}{K\left(\cos \frac{\bar{a}}{2}\right)} \{P\} \tag{51}$$

where

$$[L] = \begin{bmatrix} 1 + L_1\beta_{11} & L_2\beta_{21} & \cdots & L_N\beta_{N1} \\ L_1\beta_{12} & 1 + L_2\beta_{22} & \cdots & L_N\beta_{N2} \\ \vdots & \vdots & \vdots & \vdots \\ L_1\beta_{1N} & L_2\beta_{2N} & \cdots & 1 + L_N\beta_{NN} \end{bmatrix} \tag{52}$$

$$\{P\} = \begin{Bmatrix} P_1 \cos \bar{a}) \\ P_2(\cos \bar{a}) \\ \vdots \\ P_N(\cos \bar{a}) \end{Bmatrix} \tag{53}$$

and $\{\overline{F}\} = \{\overline{F}_1, \overline{F}_2, \ldots, \overline{F}_N\}^{\mathrm{T}}$.

From Eq. (51), the solution of $\{\overline{F}\}$ is obtained as,

$$\{\overline{F}\} = \frac{V}{K(\cos \frac{\bar{a}}{2})} [L]^{-1} \{P\} \tag{54}$$

The coefficients $\{F\} = \{F_1, F_2, \ldots, F_N\}^{\mathrm{T}}$ is thus derived from Eq. (42)

$$\{F\} = \mathrm{diag}\left(\mathrm{e}^{k_i h}(L_i + 1)\right)\{\overline{F}\} = \frac{V}{K(\cos \frac{\bar{a}}{2})} \mathrm{diag}\left(\mathrm{e}^{k_i h}(L_i + 1)\right)[L]^{-1}\{P\} \tag{55}$$

where diag(o) is the diagonal matrix which is defined as $\mathrm{diag}(z_i) = \begin{bmatrix} z_1 & 0 & \cdots & 0 \\ 0 & z_2 & \cdots & 0 \\ \vdots & \vdots & \vdots & 0 \\ 0 & 0 & 0 & z_n \end{bmatrix}$

The coefficients $\{B_1\} = \{B_{11}, B_{12}, \ldots, B_{1N}\}^{\mathrm{T}}$ and $\{B_2\} = \{B_{21}, B_{22}, \ldots, B_{2N}\}^{\mathrm{T}}$ are obtained from Eqs. (39) and (40):

$$\{B_1\} = \mathrm{diag}\left(\frac{\mathrm{e}^{-k_i h}}{J_{3i} - \frac{J_{1i}}{J_{2i}} J_{4i}}\right)\{F\} = \frac{V}{K(\cos \frac{\bar{a}}{2})} \mathrm{diag}\left(\frac{(L_i + 1)}{J_{3i} - \frac{J_{1i}}{J_{2i}} J_{4i}}\right)[L]^{-1}\{P\} \tag{56}$$

$$\{B_2\} = \mathrm{diag}\left(\frac{\mathrm{e}^{-k_i h}}{J_{4i} - \frac{J_{2i}}{J_{1i}} J_{3i}}\right)\{F\} = \frac{V}{K(\cos \frac{\bar{a}}{2})} \mathrm{diag}\left(\frac{(L_i + 1)}{J_{4i} - \frac{J_{2i}}{J_{1i}} J_{3i}}\right)[L]^{-1}\{P\} \tag{57}$$

The coefficients $\{A_1\} = \{A_{11}, A_{12}, \ldots, A_{1N}\}^{\mathrm{T}}$, $\{A_2\} = \{A_{21}, A_{22}, \ldots, A_{2N}\}^{\mathrm{T}}$ and $\{C_1\} = \{C_{11}, C_{12}, \ldots, C_{1N}\}^{\mathrm{T}}$, $\{C_2\} = \{C_{21}, C_{22}, \ldots, C_{2N}\}^{\mathrm{T}}$ will be obtained from Eqs. (22), (30), (33) and (34).

$$\{A_1\} = \frac{V}{K(\cos \frac{\bar{a}}{2})} \mathrm{diag}\left(\frac{H_{1i}(L_i + 1)}{J_{3i} - \frac{J_{1i}}{J_{2i}} J_{4i}} + \frac{H_{2i}(L_i + 1)}{J_{4i} - \frac{J_{2i}}{J_{1i}} J_{3i}}\right)[L]^{-1}\{P\} \tag{58}$$

$$\{A_2\} = \frac{V}{K(\cos \frac{\bar{a}}{2})} \mathrm{diag}\left(\frac{H_{3i}(L_i + 1)}{J_{3i} - \frac{J_{1i}}{J_{2i}} J_{4i}} + \frac{H_{4i}(L_i + 1)}{J_{4i} - \frac{J_{2i}}{J_{1i}} J_{3i}}\right)[L]^{-1}\{P\} \tag{59}$$

$$\{C_2\} = \frac{V}{K(\cos \frac{\bar{a}}{2})} \mathrm{diag}\left(\frac{1}{\mathrm{e}^{2\chi_i' h'} + 1}\left[\frac{(H_{1i} + H_{3i})(L_i + 1)}{J_{3i} - \frac{J_{1i}}{J_{2i}} J_{4i}} + \frac{(H_{2i} + H_{4i})(L_i + 1)}{J_{4i} - \frac{J_{2i}}{J_{1i}} J_{3i}}\right]\right)[L]^{-1}\{P\} \tag{60}$$

$$\{C_1\} = \frac{V}{K(\cos \frac{\bar{a}}{2})} \mathrm{diag}\left(\frac{\mathrm{e}^{2\chi_i' h'}}{\mathrm{e}^{2\chi_i' h'} + 1}\left[\frac{(H_{1i} + H_{3i})(L_i + 1)}{J_{3i} - \frac{J_{1i}}{J_{2i}} J_{4i}} + \frac{(H_{2i} + H_{4i})(L_i + 1)}{J_{4i} - \frac{J_{2i}}{J_{1i}} J_{3i}}\right]\right)[L]^{-1}\{P\} \tag{61}$$

Hence, the analytical solutions of the deflection in both the metal substrate and the piezoelectric layer, the electric potential and electric displacement in the piezoelectric layer and the vacuum can then be obtained from Eqs. (1)–(7), (12) and (13) upon obtaining the results of coefficients $\{C_1\}$, $\{C_2\}$, $\{A_1\}$, $\{A_2\}$, $\{B_1\}$, $\{B_2\}$ and $\{F\}$.

4. Analytical solution of the structure with finitely long IDT

In the foregoing session, the analytical solution for wave propagation by infinitely long IDT has been obtained. In the next part, the analytical solution for the wave propagation in the structure with finitely long IDT will be discussed.

The length of IDT is assumed to be $2L$. First the electric potential $\phi'(x_1, x_2, t)$ of the metal for $x_2 < -h$ is investigated.

The Fourier transform of the function with respect to x_1 is performed as,

$$\phi'(x_1, x_2, t) = \frac{1}{2\pi} \int_{-\infty}^{\infty} \bar{\phi}'(\xi, x_2, t) e^{-i\xi x_1} \, d\xi \tag{62}$$

The image function $\bar{\phi}'$ can be written below according to Eq. (12):

$$\bar{\phi}'(\xi, x_2, t) = \bar{\phi}'(\xi, 0, t) e^{\xi x_2} \tag{63}$$

The solution of image function of $\bar{\phi}'(\xi, x_2, t)$ requires the knowledge of the distribution of ϕ' throughout the boundary. Parton and Kudryavtser (1988) proposed an assumption that the electric potential of the vacuum for structure with finitely long IDT could be used by the solution of the electric potential of the vacuum in the structure with infinitely long IDT, when they studied the Lamb wave propagation excited by IDT without considering the piezoelectric–mechanical coupling effect. The similar assumption will be employed again in the study of wave propagation in this piezoelectric coupled plate structure with finitely long IDT below. In this paper, it is assumed that $\phi'(x_1, 0, t)$ is given by Eqs. (12) and (55), which are obtained by the solution for infinitely long IDT, in the electrodes region and null out side the electrodes region for this case. This assumption should be realistic for long transducer gratings.

In view of the above statement, we find,

$$\bar{\phi}'(\xi, 0, t) = \int_{-L}^{L} \phi'(x_1, 0, t) e^{i\xi x_1} \, dx_1 \tag{64}$$

Substituting Eq. (12) into the above equation yields,

$$\bar{\phi}'(\xi, 0, t) = \sum_{i=0}^{N} F_i \left(\frac{\sin(k_i + \xi)L}{k_i + \xi} + \frac{\sin(k_i - \xi)L}{k_i - \xi} \right) e^{i\omega t} \tag{65}$$

where F_i is expressed from Eq. (55).

Upon obtaining the distribution of the electric potential of the vacuum, the distribution of the deflection in the host metal and the piezoelectric layer, as well as the electric potential distribution in the piezoelectric layer will be discussed and obtained hereinafter.

The image functions for the Fourier transform of the variables $u_3'(x_1, x_3, t)$ in host metal, $\psi(x_1, x_3, t) = \phi(x_1, x_3, t) - (e_{15}/\Xi_{11}) u_3(x_1, x_3, t)$ and $u_3(x_1, x_3, t)$ in the piezoelectric layer with respect of x_1, similarly expressed in Eq. (62), are $\bar{u}_3'(\xi, x_3, t)$, $\overline{\psi}(\xi, x_3, t)$, and $\bar{u}_3(\xi, x_3, t)$.

Based on the detailed analyses of these variables in Part 1 of the research, the above variables can be written as follows:

$$\bar{u}_3'(\xi, x_2, t) = \left(\overline{U}_{31}'(\xi) e^{-\chi' x_2} + \overline{U}_{32}'(\xi) e^{\chi' x_2} \right) e^{i\omega t} \tag{66}$$

$$\bar{u}_3(\xi, x_2, t) = \left(\overline{U}_{31}(\xi) e^{-\chi x_2} + \overline{U}_{32}(\xi) e^{\chi x_2} \right) e^{i\omega t} \tag{67}$$

$$\overline{\psi}(\xi, x_2, t) = \left(\overline{\psi}_1(\xi) e^{-\xi x_2} + \overline{\psi}_2(\xi) e^{\xi x_2} \right) e^{i\omega t} \tag{68}$$

where

$$\chi' = \xi\sqrt{1-\left(\frac{\omega}{\xi v'}\right)^2}, \quad \chi = \xi\sqrt{\left|1-\left(\frac{\omega}{\xi v}\right)^2\right|}$$

As assumed before, the electric potential on the surface of the piezoelectric layer is the same with the electric potential in the vacuum which is shown in Eqs. (62)–(65). Therefore, the boundary conditions in the current case will be expressed by:

- Eq. (14), the continuity of the deflection at the interface;

$$\overline{U}'_{31} + \overline{U}'_{32} = \overline{U}_{31} + \overline{U}_{32} \tag{69}$$

- Eq. (15), the continuity of the stress at the interface;

$$(-\chi)\bar{c}_{44}(\overline{U}_{31} - \overline{U}_{32}) + (-\xi)\mathrm{e}_{15}(\overline{\psi}_1 - \overline{\psi}_2) = (-\chi')c'_{44}(\overline{U}'_{31} - \overline{U}'_{32}) \tag{70}$$

- Eq. (16), zero potential at the interface;

$$\overline{\psi}_1 + \overline{\psi}_2 + \frac{\mathrm{e}_{15}}{\Xi_{11}}(\overline{U}_{31} + \overline{U}_{32}) = 0 \tag{71}$$

- Eq. (17), free traction at the surface of piezoelectric layer;

$$(-\chi)\bar{c}_{44}(\overline{U}_{31}\mathrm{e}^{\chi h} - \overline{U}_{32}\mathrm{e}^{-\chi h}) + (-\xi)\mathrm{e}_{15}(\overline{\psi}_1\mathrm{e}^{\xi h} - \overline{\psi}_2\mathrm{e}^{-\xi h}) = 0 \tag{72}$$

- Eq. (18), continuity of electric potential with the vacuum;

$$\left(\overline{\psi}_1\mathrm{e}^{\xi h} + \overline{\psi}_2\mathrm{e}^{-\xi h}\right) + \frac{\mathrm{e}_{15}}{\Xi_{11}}(\overline{U}_{31}\mathrm{e}^{\chi h} + \overline{U}_{32}\mathrm{e}^{-\chi h}) = \bar{\phi}'(\xi,0,t)\mathrm{e}^{-\xi h} \tag{73}$$

- Eq. (21), free traction at the lower surface of the metal core;

$$\overline{U}'_{31}\mathrm{e}^{\chi' h'} - \overline{U}'_{32}\mathrm{e}^{-\chi' h'} = 0 \tag{74}$$

In Part 1 of the paper, the dispersion characteristics are obtained by studying a homogeneous solution, i.e. zero potential at the surface of the piezoelectric layer, whereas in the current study, the particular solution is to be search as $\bar{\phi}' \neq 0$ in Eq. (73). The solutions for $\overline{U}'_3$, $\overline{U}_{31}$, $\overline{U}_{32}$, $\overline{\psi}_1$ and $\overline{\psi}_2$ will be obtained below.

Similar to the dispersion characteristic analysis of the structure in Part 1, $\overline{\psi}_1$ and $\overline{\psi}_2$ can be expressed in terms of $\overline{U}'_{31}$ and $\overline{U}'_{32}$ from Eqs. (69)–(71), as

$$\overline{\psi}_1 = \frac{1}{2}\left(X - \frac{\mathrm{e}_{15}}{\Xi_{11}}\right)\overline{U}_{31} + \frac{1}{2}\left(Y - \frac{\mathrm{e}_{15}}{\Xi_{11}}\right)\overline{U}_{32} \tag{75}$$

$$\overline{\psi}_2 = \frac{1}{2}\left(-X - \frac{\mathrm{e}_{15}}{\Xi_{11}}\right)\overline{U}_{31} + \frac{1}{2}\left(-Y - \frac{\mathrm{e}_{15}}{\Xi_{11}}\right)\overline{U}_{32} \tag{76}$$

where

$$X = \frac{\mathrm{e}^{2\chi' h'} - 1}{\mathrm{e}^{2\chi' h'} + 1}\frac{c'_{44}}{\mathrm{e}_{15}}\sqrt{1-\left(\frac{\omega}{\xi v'}\right)^2} - \frac{\bar{c}_{44}}{\mathrm{e}_{15}}\sqrt{\left|1-\left(\frac{\omega}{\xi v}\right)^2\right|}$$

$$Y = \frac{\mathrm{e}^{2\chi' h'} - 1}{\mathrm{e}^{2\chi' h'} + 1}\frac{c'_{44}}{\mathrm{e}_{15}}\sqrt{1-\left(\frac{\omega}{\xi v'}\right)^2} + \frac{\bar{c}_{44}}{\mathrm{e}_{15}}\sqrt{\left|1-\left(\frac{\omega}{\xi v}\right)^2\right|}$$

Substituting $\overline{\psi}_1$ and $\overline{\psi}_2$ into Eqs. (72) and (73), we have,

$$\left\{\frac{1}{2}\left(X-\frac{e_{15}}{\Xi_{11}}\right)e^{\xi h}-\frac{1}{2}\left(-X-\frac{e_{15}}{\Xi_{11}}\right)e^{-\xi h}+Ze^{\chi h}\right\}\overline{U}_{31}+\left\{\frac{1}{2}\left(Y-\frac{e_{15}}{\Xi_{11}}\right)e^{\xi h}-\frac{1}{2}\left(-Y-\frac{e_{15}}{\Xi_{11}}\right)e^{-\xi_1 h}-Ze^{-\chi h}\right\}\overline{U}_{32}=\Delta_1\overline{U}_{31}+\Delta_2\overline{U}_{32}=0 \tag{77}$$

$$\left\{\frac{1}{2}\left(X-\frac{e_{15}}{\Xi_{11}}\right)e^{\xi h}+\frac{1}{2}\left(-X-\frac{e_{15}}{\Xi_{11}}\right)e^{-\xi h}+\frac{e_{15}}{\Xi_{11}}e^{\chi h}\right\}\overline{U}_{31}+\left\{\frac{1}{2}\left(Y-\frac{e_{15}}{\Xi_{11}}\right)e^{\xi h}+\frac{1}{2}\left(-Y-\frac{e_{15}}{\Xi_{11}}\right)e^{-\xi h}+\frac{e_{15}}{\Xi_{11}}e^{-\chi h}\right\}\overline{U}_{32}=\Delta_3\overline{U}_{31}+\Delta_4\overline{U}_{32}=\bar{\phi}'(\xi,0)e^{-\xi h} \tag{78}$$

where

$$Z=\tfrac{1}{2}(Y-X),\quad \bar{\phi}'(\xi,0)=\sum_{i=0}^{N}C_i\left(\frac{\sin(k_i+\xi)L}{k_i+\xi}+\frac{\sin(k_i-\xi)L}{k_i-\xi}\right)$$

From Eqs. (77) and (78), we obtain the solution of $\overline{U}_{31}$, $\overline{U}_{32}$ as,

$$\overline{U}_{31}=-\frac{\bar{\phi}'(\xi,0)e^{-\xi h}\Delta_2}{\Delta} \tag{79}$$

$$\overline{U}_{32}=-\frac{\bar{\phi}'(\xi,0)e^{-\xi h}\Delta_1}{\Delta} \tag{80}$$

where $\Delta=\Delta_2\Delta_3-\Delta_1\Delta_4$, which is exactly the determinant of dispersion characteristics of the SH wave in this piezoelectric plate obtained in Part 1.

$\overline{\psi}_1$ and $\overline{\psi}_2$ can be obtained from Eqs. (75) and (76) when substituting the above solutions.

$$\overline{\psi}_1=\frac{1}{2}\frac{\bar{\phi}'(\xi,0)e^{-\xi h}}{\Delta}\left(\left(X-\frac{e_{15}}{\Xi_{11}}\right)\Delta_2-\left(Y-\frac{e_{15}}{\Xi_{11}}\right)\Delta_1\right) \tag{81}$$

$$\overline{\psi}_2=\frac{1}{2}\frac{\bar{\phi}'(\xi,0)e^{-\xi h}}{\Delta}\left(\left(-X-\frac{e_{15}}{\Xi_{11}}\right)\Delta_2-\left(-Y-\frac{e_{15}}{\Xi_{11}}\right)\Delta_1\right) \tag{82}$$

$\overline{U}_3'$ is obtained from Eq. (66) as,

$$\bar{u}_3'=\frac{\bar{\phi}'(\xi,0)e^{-\xi h}}{(e^{2\chi' h'}-1)\Delta}(e^{-\chi' x_2}+e^{2\chi' h'}e^{\chi' x_2})(\Delta_2-\Delta_1) \tag{83}$$

Thus the deflection in the host metal, $u_3'(x_1,x_3,t)$, is finally derived after Fourier transform,

$$u_3'(x_1,x_2,t)=\frac{1}{2\pi}\int_{-\infty}^{\infty}\frac{\bar{\phi}'(\xi,0)e^{-\xi h}}{\Delta}(\Delta_2-\Delta_1)\frac{(e^{-\chi' x_2}e^{2\chi' h'}+e^{\chi' x_2})}{(e^{2\chi' h'}-1)}e^{i\omega t}e^{-i\xi x_1}\,d\xi \tag{84}$$

The above improper integration can be discussed by the residue theorem.

A single pole in the complex integrand of the last equation is, ξ_s, i.e. the root of the following equation,

$$\Delta=0 \tag{85}$$

The integration of the complex function is along a close path which comprises a curve with radius R in the upper half plane and the real axis. Note that the exponential characteristic of Δ is the order of $e^{2\xi h}$, which ensures the integration null along the curve in the upper half plane as $R\to\infty$. Thus, the solution for the improper integration of Eq. (84) is obtained as,

$$u_3'(x_1,x_2,t)=\frac{\mathrm{i}}{2}\frac{\bar{\phi}'(\xi_s,0)\mathrm{e}^{-\xi_s h}}{\Delta'\big|_{\xi=\xi_s}}(\Delta_2-\Delta_1)|_{\xi=\xi_s}\frac{(\mathrm{e}^{-\chi' x_2}\mathrm{e}^{2\chi' h'}+\mathrm{e}^{\chi' x_2})}{(\mathrm{e}^{2\chi' h'}-1)}\Bigg|_{\xi=\xi_s}\exp(\mathrm{i}(\omega t-\xi_s x_1)) \tag{86}$$

It is noted that Eq. (85) is the dispersion characteristic equation of the piezoelectric coupled plate discussed in Part 1. The dispersion curve of the structure and the corresponding mode shapes of SH wave propagation have already been obtained. As is concluded in Part 1, the first wave mode is the Bleustein–Gulyayev surface wave propagation, such surface wave propagation can thus be excited by use of IDT from the above analytical solution by choosing value of ξ_s from the dispersion curve at the fixed frequency ω in the dispersion curves.

The deflection in the piezoelectric layer is similarly obtained by Eqs. (2), (67), (79) and (80) after manipulating Fourier transform as,

$$u_3(x_1,x_3,t)=\frac{\mathrm{i}}{2}\frac{\bar{\phi}'(\xi_s,0)\mathrm{e}^{-\xi_s h}}{\Delta'\big|_{\xi=\xi_s}}(\Delta_1\mathrm{e}^{-\chi x_2}-\Delta_2\mathrm{e}^{\chi x_2})|_{\xi=\xi_s}\exp(\mathrm{i}(\omega t-\xi_s x_1)) \tag{87}$$

The solution for $\psi(x_1,x_3,t)$ is obtained from Eqs. (68), (75) and (76) as follows,

$$\begin{aligned}\psi(x_1,x_3,t)=\frac{\mathrm{i}}{4}\frac{\bar{\phi}'(\xi_s,0)\mathrm{e}^{-\xi_s h}}{\Delta'\big|_{\xi=\xi_s}}&\left(\left(\left(X-\frac{\mathrm{e}_{15}}{\Xi_{11}}\right)\Delta_2-\left(Y-\frac{\mathrm{e}_{15}}{\Xi_{11}}\right)\Delta_1\right)\mathrm{e}^{-\xi x_2}\right.\\&\left.+\left(\left(-X-\frac{\mathrm{e}_{15}}{\Xi_{11}}\right)\Delta_2-\left(-Y-\frac{\mathrm{e}_{15}}{\Xi_{11}}\right)\Delta_1\right)\mathrm{e}^{\xi x_2}\right)\Bigg|_{\xi=\xi_s}\exp(\mathrm{i}(\omega t-\xi_s x_1))\end{aligned} \tag{88}$$

The electric potential in the piezoelectric layer can be expressed from Eq. (4). This electric potential has been assigned to be the same with that in the vacuum which, by the assumption, is by the results for the structure with infinitely long IDT. Thus the analytical solutions for the SH wave propagation in this piezoelectric coupled structure are finally obtained. The solution reveals that the wave propagation in this piezoelectric coupled plate bonded by IDT is just the surface wave propagation whose characteristics are obtained in Part 1 of the paper, and the magnitude of the solution are derived accordingly in this part of research.

5. Concluding remarks

The analytical solution for the SH wave propagation excited IDT in a piezoelectric coupled plate are obtained in Part 2 of the research paper. The analysis is based on the surface wave solution obtained in the Part 1 of the paper. The solution is first attempted for the case when infinitely long IDT is used in the structure. The wave number of the wave propagation is assumed to be big enough for the derivation of the mathematical solution of this structure. This hypothesis of the wavelength of IDT is discussed by standard steel-PZT and gold-PZT structures, and the results show that the hypothesis can be satisfied according to the usual design of the IDT wavelength. The solution for the wave propagation by finitely long IDT is obtained by using Fourier transform. The distribution of the electric potential in the vacuum in this case is assumed to be the distribution obtained for the case of infinitely long IDT. The solution from the paper also reveals that the wave propagation in this piezoelectric coupled plate bonded by IDT is just the surface wave propagation whose characteristics are obtained in Part 1 of the paper, and the magnitude of the solution are derived accordingly in this paper.

The potential of the research lies in the application of IDT in the excitation of all type of waves in all kinds of structures surface bonded by the piezoelectric layer. One of the applications is in the health monitoring of structures by the wave propagation signals. Further work will be focused on the design of the

IDT and its applications. Besides, other types of wave propagations, such as Lamb wave, are also needed to be investigated for the application of piezoelectric coupled structures with IDT.

Acknowledgements

The work in this paper is partly supported by the research grant from National University of Singapore, R-264-000-113-112.

References

Auld, B.A., 1973a. Acoustic Fields and Waves in Solids Volume I. Wiley, New York.

Auld, B.A., 1973b. Acoustic Fields and Waves in Solids Volume II. Wiley, New York.

Badcock, R.A., Birt, E.A., 2000. The use 0–3 of piezocomposite embedded Lamb wave sensors for detection of damage in advanced fibre composites. Smart Mater. Struct. 9, 291–297.

Balakrirev, M.K., Gilinskii, I.A., 1982. Waves in Piezocrystal. Nauka, Novosibirsk.

Bateman, H., Erdelyi, A., 1955. Higher Transcendental Functions. McGraw-Hill, New York.

Campbell, C.K., 1998. Surface Acoustic Wave Devices for Mobile and Wireless Communications. New York, Academic.

Coquin, G.A., Tierstan, T.E., 1967. Analysis of the excitation and detection of piezoelectric surface waves in quartz by means of surface electrodes. J. Acoust. Soc. Am. 41, 921–939.

Hasegawa, K., Koshiba, M., 1990. Finite-element solution of Rayleigh-wave scattering from reflective gratings on a piezoelectric substrate. IEEE Trans. Ultrason. Ferroelectr. Freq. Control 37, 99–105.

Joshin, S.G., White, R.M., 1969. Excitation and detection of surface elastic waves in piezoelectric crystals. J. Acoust. Soc. Am. 46, 17–27.

Milsom, R.F., Reilly, N.H.C., Redwood, M., 1977. Analysis of generation and detection of surface and bulk acoustic waves by interdigital transducer. IEEE Trans. Sonics Ultrason SU-24, 147–166.

Monkhouse, R.S.C., Wilcox, P.W., Dalton, R.P., Cawley, P., 2000. The rapid monitoring of structures using interdigital Lamb wave transducers. Smart Mater. Struct. 9, 304–309.

Morgan, D.P., 1985. Surface Wave Devices for Signal Processing. Elsevier, Amsterdam.

Morgan, D.P., 1998. History of SAW devices. IEEE Int. Freq. Contr. Symp. 439–460.

Ogilvy, J.A., 1996. An approximate analysis of waves in layered piezoelectric plates from an interdigital source transducer. J. Phys. D. Appl. Phys. 29(3), 876–884.

Parton, V.Z., Kudryavtser, B.A., 1988. Electromagnetoelasticity. Gordon and Breach, New York.

Tseng, G.C., 1968. Frequency response of an interdigital transducers for excitation of surface elastic waves. IEEE Trans. Electron Dev. EQ-15, 586–594.

Varadan, V.K., Varadan, V.V., 2000. Microsensors, microelectromechanical systems (MEMS), and electronics for smart structures and systems. Smart Mater. Struct. 9, 953–972.

Ventura, P., Hode, J.M., Sodal, M., 1995. A new efficient combined FEM and periodic Green's function formalism for analysis of periodic SAW structures. Proc. IEEE Ultrason. Symp. 263–268.

White, R.M., 1998. Acoustic sensors for physical, chemical, and biochemical application. IEEE Int. Freq. Contr. Symp. 587–594.

Xu, G.S., 2000. Direct finite-element analysis of the frequency response of a Y–Z lithium niobate SAW filter. Smart Mater. Struct. 9, 973–980.

Yong, Y.K., Garon, R., Kanna, S., Hashimoto, K.Y., 1998. Effects of periodically missing fingers and periodically shifted fingers on SAW propagation in quartz resonators. IEEE Int. Freq. Contr. Symp. 461–469.

Zhang, Y., Desbois, J., Boyer, L., 1993. Characteristic parameters of surface acoustic waves in a periodic metal grating on a piezoelectric substrate. IEEE Trans. Ultrason. Ferroelectr. Freq. Contr. UEFC-40, 183–192.